Rapid ion beam induced Ostwald ripening in two dimensions

P. Berdahl, R. P. Reade, and R. E. Russo

Environmental Energy Technology Division

Lawrence Berkeley National Laboratory

Berkeley, CA 94720

Ion beam induced grain coarsening in initially amorphous $(Zr,Y)O_x$ layers is observed by atomic force microscopy. The films were bombarded at room temperature. Grain boundary grooves indicate that the larger grains have a diameter of about 83 nm at 2 min, and 131 nm at 5 minutes. Up to 5 minutes, the grain size evolves with time as t^{β}, with $\beta = 0.5 \pm 0.2$. Based on a new parametrization of ion-induced grain boundary translation, we derive a theoretical estimate of $\beta = 3/7$, consistent with our measurement. By 7.5 minutes, many of the grain boundary grooves are shallow and indistinct, suggesting that the surviving grains are mutually well aligned. Such rapid grain growth at room temperature is unusual, and is enabled by the ion bombardment. Similar grain growth processes are expected during ion beam assisted deposition film growth. The status of ion textured yttria stabilized zirconia (YSZ) films as buffer layers for high-current high-temperature superconducting films is briefly summarized.

Preprint submitted to J. Appl. Phys. 30 June 2004.

Introduction

Classical Ostwald ripening occurs during chemical precipitation from solution. Small crystallites are less stable than larger ones, due to their larger surface to volume ratio. They tend to dissolve and ultimately contribute mass to the larger crystallites. Thus, the mean crystallite size increases with time. Very similar phenomena occur when polycrystalline materials are annealed. Grain boundaries contribute a positive energy per unit area that is reduced by the process of grain coarsening. Corresponding two-dimensional grain growth can occur in thin films, at the surface of thin films, and in monolayers.

The motion of a grain boundary that reduces its curvature and area is governed by the grain boundary mobility. In the case at hand, the grain boundary energy per unit area may attain a typical value for a polycrystalline material, but the grain boundary mobility is greatly enhanced over mere thermal activation, due to the effect of ion bombardment. For the simple theoretical case of a two-dimensional soap froth, analysis shows that grains with more than six neighbors grow, while grains with fewer than six neighbors shrink.[1,2] A more detailed theoretical analysis,[3] in which the grain boundaries are replaced by a small amount of a liquid solvent phase, suggests that the mean grain size R should for long times t evolve as $R = k\, t^{\beta}$, with coefficient k and growth exponent β. Fan *et al.*[3] find that the coefficient k is sensitive to the volume fraction of the solid phase, but that β is consistently 1/3 for two-dimensional thermal annealing.

The deposition of fully-oriented ("biaxially textured") crystalline films on technical substrates such as glass and polycrystalline metal has important practical applications. For example, the oblique ion beam assisted deposition (IBAD) of YSZ films on metal substrates has led to methods for synthesizing high-current tapes of the high temperature superconductor $YBa_2Cu_3O_7$ (YBCO) [4-6] It is not difficult to envisage further potential applications of biaxial ion texturing of films for photovoltaics, magnetoresistance, flat panel displays, catalysis, sensors, etc.

Film synthesis by physical vapor deposition is still an empirical art. For example, process optimizations routinely include variations in parameters such as partial pressure of reactant species and substrate temperature, since the best conditions are not known *a priori*. Better fundamental understanding of film synthesis is clearly needed. One strategy for isolating specific phenomena occurring during film growth is to examine amorphous films. These films can be free of some complications of polycrystalline film growth, such as crystalline anisotropy. For example, studies of stress during silicon and germanium film growth are more readily interpreted when the amorphous phase is synthesized.[7]

The system we study here is initially amorphous; it also could be classed as nanocrystalline. (The $\theta/2\theta$ diffraction pattern has only a very broad peak at 34.2˚, with FWHM of 4.0˚.) Under the influence of the ion beam, dense grains nucleate, grow to mutual impingement, coarsen, and ultimately coalesce.

Background

Ion texturing is the phenomenon in which oriented crystals form in the surface region of a film, due to oblique ion bombardment. It is performed under conditions similar to IBAD, but there is no concurrent film vapor deposition. Therefore, it may help us to understand the more complex IBAD processes. High temperature (800 ˚C) ion texturing of YSZ led to a {001}<110> surface texture that is suitable for YBCO deposition, but difficult to reproduce due to premature spontaneous crystallization.[8] (Here, the notation lists, first the crystallographic orientation normal to the film, and second, the orientation in the plane of the film along the direction of the projection of the ion beam.) This geometry is the same as for conventional room temperature IBAD processing of YSZ, in which the 55˚ ion beam is parallel to a (111) crystal direction. Bombardment of oxygen deficient amorphous YSZ at an intermediate temperature (250 ˚C) in one experiment yielded an in-plane oriented film with (111) fiber texture. Bombardment at room temperature of oxygen deficient amorphous YSZ films results in a {211}<111> texture.[9] In this process, a low-index direction of the crystal lattice is not aligned with the ion beam. Increasing the temperature during bombardment results in epitaxial oxidation and growth of the {211}<111> texture down through the bulk of the film. In an effort to clarify the nature of the {211}<111> process, we are here investigating the effects of ion texturing at room temperature by examination of the resulting grain boundary grooves. We will not attempt to analyze grain nucleation and early growth here; this subject is left for future investigation.

The effects of low-energy (300 eV) oblique Ar ion impacts are localized. Estimates with the SRIM program[10] suggest that most of the ion energy is dissipated in a depth of about 1 nm and in a volume of roughly 1 nm^3. Zr and Y atoms struck head on by incoming ions can reach energies up to about 130 eV and these can also penetrate a nanometer or so into the film. Ion impacts also cause both transverse and longitudinal phonon emission, and a thermal spike, that can affect the local microstructure.

Preferential sputtering of oxygen at the surface occurs, but the sputtered oxygen is largely replaced by reaction with activated ambient oxygen. (Under IBAD growth using the same oxygen pressure, fully oxygenated YSZ films are formed.) Due to sputtering of the cations, we expect that the surface recedes at a rate of roughly 0.05 nm s^{-1}, based on our IBAD experience. Ressler *et al*.[11] report ion etch rates for YSZ crystals as about 0.024 nm s^{-1} at 95 μA cm^{-2} (300 eV, 45 deg. incidence), which translates to about 0.1 nm s^{-1} for our ion current. Dzick *et al*.[12] report ion etch rates (without citing ion current) for YSZ crystals and films in the range of 0.05 to 0.07 nm s^{-1}, with the highest rate for amorphous films.

Experiment

The precursor films were deposited by reactive magnetron sputtering of a $Zr_{0.82}Y_{0.18}$ target in the presence of oxygen onto a rolled metal substrate.[9] They contain only about half the oxygen of fully oxidized YSZ, are electrical conductors, and are x-ray amorphous. The metal substrates are smooth on a scale of a few nanometers, but contain

many linear corrugations due to the rolling process. The bombardment conditions were 300 eV Ar^+ ions (400 μA cm^{-2}, ion flux of 2.5 x 10^{15} cm^{-2} s^{-1}), 55° from the film normal, in the presence of 0.4 mtorr of O_2 and 0.4 mtorr of Ar.

Figure 1 shows the surface topography of a sample that was bombarded for only 30 sec at room temperature, followed by rapid heating to several hundred degrees to fully oxidize the film. The total time of ion bombardment was 3 min. The 5 x 5 micrometer image shows the many linear features that are artifacts caused by the underlying rolling marks in the substrate, and also shows the presence of numerous dome-like features, that resemble the surface of grains observed in polycrystalline films. The accompanying 1 x 1 micrometer image of a relatively uniform part of the same sample shows more detail. Some acoustic noise (short wavelength ripple) is also present. Analysis of an unbombarded precursor film also showed rolling mark artifacts. A selected uniform 250 nm x 400 nm section of the untreated sample had a measured surface roughness of 0.8 nm rms, partly due to the acoustic noise. Thus, the unbombarded film did not show the grain structure evident in Fig. 1.

In order to investigate the development of the film grain structure, three samples were bombarded at room temperature for 2, 5 and 7.5 minutes, respectively, without heating. Topographs are shown in Fig. 2. Some features due to the corrugated substrate can be seen; these are aligned with the left edge of the figures. It seems clear from the data, however, that the surface consists of smooth domes, separated by grain boundary grooves, and that bombardment causes grain growth.

Sectional profile analysis was performed to estimate the grain dimensions. The grain diameter is roughly 83 nm at 2 min. and 131 nm at 5 min., based on the median size of a number of the larger grains. Due to the indistinct nature of the grain boundaries in Fig. 2(c) (7.5 min), the grain size was not estimated. The background of figure 2(d) shows a particularly large grain found in the 7.5 min. sample (diameter, about 380 nm, height about 13 nm); the foreground shows additional indistinct grain boundaries. We can make a rough estimate of the growth exponent β using the sizes 0, 81, and 131 nm at times of 0, 2, and 5 minutes: $\beta = 0.5 \pm 0.2$, where the uncertainty is due to size measurement errors (limited statistics) and the possibility that all the grain boundaries may not have been detected. We attribute the unusually large grain in Fig. 2 (d) to coalescence of a number of subgrains, since it is too large to have been formed merely by coarsening.

The median slope β_s of the grains near the grain boundaries was found to be about 7.2º at 2 min. and 6.8º at 5 min. At 7.5 min, the (uncertain) slopes were found to be roughly 3.4º. The surfaces of the grains in Fig. 2 appear smooth, suggesting that the ion-induced mobility of surface atoms is high. The lack of faceting also suggests that the surface energy γ_s is roughly isotropic. The grain boundary energy can be estimated as $\gamma_b = 2 \gamma_s \sin(\beta_s)$, due to the balance of the tensions where the boundary meets the surface, as discussed by Mullins.[13] Thus we have $\gamma_b/\gamma_s = 0.24$ at 2 and 5 min., and $\gamma_b/\gamma_s \sim 0.12$ at 7.5 min.

In situ reflection high energy electron diffraction (RHEED) data do not show a crystalline spot pattern; rather they show an "amorphous" glow that indicates that the surface of the grains is disordered.

Discussion

Of what are the grains composed? We believe the most likely possibility is that they are thin ion-damaged crystallites with disordered surfaces. The strongest direct evidence we have for crystallinity is that epitaxial oxidation of the ion textured film at elevated temperatures produces a distinct {211}<111> texture throughout, and epitaxial growth of CeO_2 at 500 ˚C on top of an ion textured sample also produces a {211}<111> film.[9]

Grain nucleation has not yet been observed directly. If grain nucleation is an efficient process, a (roughly) 1 nm^3 volume nucleus could be produced by a single impact. At the ion impact rate of 2.5 x 10^{15} cm^{-2} s^{-1}, each 1 nm surface cube receives about 25 ions s^{-1}, so that even if nucleation requires several impacts, the surface should be covered with nuclei in a time on the order of one second. During and shortly after nucleation, we expect that the oblique bombardment may cause rotation of the individual grains but that this process becomes improbable as the grains enlarge. After the growing nuclei impinge on one another, competitive grain growth (coarsening, i.e., Ostwald ripening) occurs.

Conventionally, grain coarsening of solids requires elevated annealing temperatures. Annealing polycrystalline YSZ, for example, has little effect on the grain structure below

800 ˚C. However, we are observing rapid grain coarsening at room temperature. We propose that the mechanism is ion damage. Of the various grains, some are better oriented to resist ion damage than others. The favorably oriented grains then grow epitaxially into adjacent more-damaged grains. A mechanism of this type has been proposed by Dong and Srolovitz to explain how well-oriented grains can consume adjacent grains during molecular dynamics simulations of IBAD growth of aluminum films.[14]

Theoretical model of ion beam induced grain coarsening

We consider a simplified model of ion beam induced grain growth. When the ion beam is turned on, there is a transient (on the order of 1/25 of a second in our system) during which damage accumulates in the crystalline grains. After this transient, the grain boundaries move with velocities

$$v_{ij} = C F (q_i - q_j). \quad (1)$$

The indices i and j label the N_o initial grains with uniform initial radius R_o, C is a constant, F is the ion flux (ions cm^{-2} s^{-1}), and the set of $\{q_i\}$ are fixed numbers, "quality factors" $0 \leq q_i \leq 1$ that express the ability of the grains to resist damage by the ion beam. Note that this postulated mechanism for grain boundary translation is distinct from the conventional mechanisms discussed in the introduction that act to reduce grain boundary curvature. Therefore, even planar boundaries will move. Grains with q_i near one are

fated to grow at the expense of the others and eventually dominate the film texture. In the remainder of this section, we will consider several, increasingly likely, possibilities for the dynamics of grain growth.

Suppose, for the sake of argument, that the q_i are uniformly distributed between zero and unity at zero time, a sort of random texture. We could perform a detailed simulation of grain evolution with Eq.(1), but here we simply note the asymptotic behavior. At some later time t, most of the grains with small q_i have reached zero size. The remaining values of q_i, are distributed in a narrow interval Δq wide near unity. The number of remaining grains is $N_o \Delta q$. At this point the average (mean field) value of q of the remaining grains is about 1- $\Delta q/2$, and the rate of growth of the largest (q=1) grains is v = $C F \Delta q/2$. Assuming a circular shape for the grains, one then has

$$dR/dt = 0.5\, C F (R_o^2/R^2).$$

Integration yields

$$R = [\, R_o^3 + (3/2)\, C F R_o^2\, t]^{1/3}, \quad (2)$$

which indicates that the grain size grows like $t^{1/3}$ for long times. Grain growth is a "survival of the fittest" phenomenon in which grain growth slows down over time, due to the improving quality of the population. Many grains grow initially, only to be eventually overtaken by the stiffer competition. A more complete discussion of the grain

coarsening phenomenon would have to include the effects of the ion-induced grain boundary mobility. This mobility, driven by the energy per unit area of the grain boundaries, may be responsible for the tendency of the grains to assume a circular shape. It is interesting to note that in samples that have been heated (e.g., Fig. 1), we expect that the grain boundaries have grown down from the surface as the film is oxidized, likely pinning the grain boundaries, and the grains have a less-circular appearance.

For a slightly more realistic view of the nature of the dynamics of coarsening, we can examine the specific case when the nucleation causes a strong fiber texture (a specific crystallite orientation is always normal to the surface) and the initial in-plane orientation is random. Then the quality factor q is a function of in-plane orientation angle φ: $q = 1 - a\,(\varphi - \varphi_o)^2$. Here it has been assumed that the maximum value for q occurs at $\varphi = \varphi_o$, that after some time, only values of φ near φ_o are important, and that q is an analytic function of φ. (In our initial example q was not an analytic function of φ.) In this case, there is a relatively larger population of grains with q near one, and the asymptotic growth of grain size is proportional to $t^{1/5}$:

$$R = [R_o^5 + (5/3)\,\pi^2\, a\, C\, F\, R_o^4 t]^{1/5}, \qquad \text{(1 angle varying).} \quad (3)$$

The width of the corresponding asymptotic angular distribution $\Delta\varphi$ is proportional to $(aCFt/R_o)^{-2/5}$. However, since we have observed a growth exponent of 0.5 ± 0.2, the exponent 1/5 is not compatible with the observations. We therefore rule out the

possibility of a strong fiber texture produced by nucleation, and progress now to a more realistic model.

The complete specification of crystallite orientation requires three angles (Euler angles). If the initial population of crystallites contains all orientations, then the quality factor has the form $q = 1 - a\,(\varphi - \varphi_o)^2 - b\,(\theta - \theta_o)^2 - c\,(\chi - \chi_o)^2$ near the maximum at $q = 1$. (If cross terms appear in this formula, they can be eliminated by a suitable linear transformation to different angular variables. The full function $q(\varphi, \theta, \chi)$ depends both on the crystallite orientation with respect to the ion beam and, due to strain and surface energy effects, on the crystallite orientation with respect to the film surface.) As before, we have that $R_o^2/R^2 = N/N_o$ = ratio of final to initial occupied volume in angular configuration (φ, θ, χ) space:

$$N/N\mathrm{o} = (4/\pi)\,(abc)^{-1/2}\,(1-q_{min})^{3/2}. \qquad (4)$$

Here q_{min} is the value of q dividing the surviving grains from those that have reached zero size. The surviving grains reside in an ellipsoid of φ, θ, χ space near $(\varphi_o, \theta_o, \chi_o)$. For Eq. (4), the initial volume in the angular space was taken as $\pi^2/3$. This represents the solid angle of a sphere (4π, for two angles) times 2π for an additional rotation angle, divided by 24, the number of different ways a cube can be placed in a standard position. Thus, we are accounting for the fact that the fully oxygenated crystalline YSZ material has cubic symmetry. Equation (4) can also be written in the form

$$N/N\mathrm{o} = (4/\pi)\,\Delta\varphi\;\Delta\theta\;\Delta\chi\,, \quad (5)$$

where $\Delta\varphi$, $\Delta\theta$, and $\Delta\chi$ are the three radii of the ellipsoid in angular space, and are the half widths of the angular distributions. Note that Eq. (5) shows rather directly that the number of surviving grains is proportional to the remaining occupied volume of the angular configuration space. To estimate the rate of growth of the grains, we compute the average value of q (q_{ave}) and find that $1- q_{ave} = (3/5)(1- q_{min})$. We then have from Eq.(1) that

$$dR/dt = C F (3/5)(1- q_{min}).$$

Eliminating $(1- q_{min})$ in favor of R and integrating, we obtain

$$R^{7/3} = R_o^{7/3} + (7/5)(\pi/4)^{2/3} C F (abc)^{1/3} R_o^{4/3} t.$$

Thus we obtain (for $R >> R_o$)

$$R/R_o = (7/5)^{3/7} (\pi/4)^{2/7} (abc)^{1/7} (C F t /R_o)^{3/7}, \quad (6)$$

demonstrating that the grain radius R is proportional to $t^{3/7} = t^{0.43}$. Now, an order of magnitude estimate may be made for the constant C. Assuming that R_o is roughly 1 nm and that the factor $(abc)^{1/7}$ is roughly unity we use the observed grain radius (66 nm at 5 min) to find that C is about 2 nm^3. The ion flux is $F = 25\ nm^{-2}\ s^{-1}$, so the maximum possible grain boundary velocity CF just after nucleation (see Eq. (1)) is on the order of

50 nm s^{-1}. During the period of our observations, this velocity is much smaller, on the order of 0.1 nm s^{-1}. Still, the rate of film deposition in IBAD processing is a comparable rate, so that ion induced grain boundary translation is likely to be important during IBAD processing.

In the introduction, we pointed out that for two-dimensional grain coarsening, we might expect the growth exponent to be 1/3. However, if two mechanisms are proceeding in parallel, the larger value (here 3/7) may be expected to eventually control the growth.

The angular widths of the orientation distribution depend on the parameters *a, b*, and *c* introduced above. We find (for $R >> R_o$) that

$$\Delta\varphi = (\pi/4)^{1/7} (5/7)^{2/7} a^{-3/7} b^{1/14} c^{1/14} (CFt/R_o)^{-2/7}, \qquad (7)$$

with analogous expressions for $\Delta\theta$ and $\Delta\chi$ (permutating *a*, *b*, and *c*). Given the $t^{-2/7}$ time dependence here, the halving of $\Delta\varphi$ requires a factor of $2^{7/2} = 11.3$ times more time. For a rough estimate, we take $a = b = c = 1$ and find that at 2 min $\Delta\varphi \approx 4.1$ deg, and at 7.5 min $\Delta\varphi \approx 2.9$ deg. Since we cannot expect *a*, *b*, and *c* to be equal, these distribution half widths are lower bounds for the widest of the three angular distributions.

For completeness, we note in passing that if we regard one angle as fixed, and two angles as variable, we find

$R \approx t^{1/3}$ (2 angles varying). (8)

In most applications of ion texturing, we expect that epitaxial crystalline films will be deposited on the textured surface. It is now well established from work on IBAD films[15] that the deposited layer can have more tightly aligned crystallites than the textured surface. To enhance this effect it is advantageous to deposit films composed of crystallites that are larger than those in the ion textured layer, to encourage "averaging" of the underlying alignment. Thus we can anticipate that in applications there will be an optimum ion texturing time, for which the advantage of better crystallite orientation is offset by the disadvantage of larger crystallite size.

Status of ion textured YSZ layers as buffers for YBCO deposition

The {211} <111> YSZ texture in the current process is expected eventually to form a template for deposition of high-current films of $YBa_2Cu_3O_7$. In our prior work we used a CeO_2 buffer layer and found that the YBCO c-axis was tilted from the normal.[9] Recently, we were able to deposit YBCO directly on the {211} <111> YSZ surface, which resulted in c-axis normal films as shown in Fig. 3. However, the degree of in-plane texture shown in Fig 3 (b) is not yet adequate to support high critical currents. Further improvements needed are (i) a smoother metal substrate, (ii) sharper texture in the YSZ layer, and, especially, (iii) design of a suitable buffer layer stack that further sharpens texture and that can support a well-oriented c-axis YBCO film. The prospects for high-current YBCO films seem bright, in view of recent successes with the inclined

substrate deposition (ISD) method.[16, 17] In fact, in the Argonne work,[17] an intermediate layer in the buffer stack is in fact a {211} <111> YSZ layer.

Conclusions

In conclusion, we have studied the rapid ion-beam-induced grain coarsening in YSZ films by atomic force microscopy and found that well-oriented grains rapidly grow at the expense of others. Initial boundary motion is extrapolated to be on the order of 50 nm s^{-1}. The larger grain radii grow with an asymtotic time dependence of t^{β}. Theoretically, we estimate that $\beta = 3/7$, consistent with the experimental value of 0.5 ± 0.2. The widths of the angular distributions scale as $t^{-2/7}$. The rapid grain coarsening we have observed by ion texturing is likely to be occurring in some IBAD processes, in which it may be obscured by the simultaneous film deposition.

Albert Park assisted with the AFM measurements. John Clarke and Mark Levine provided advice and encouragement. This work was supported by the Office of Electric Transmission and Distribution, U. S. Dept. of Energy, under Contract No. DE-AC03-76SF00098.

References

1. Von Neumann J. In: Metal Interfaces. American Society for Testing Materials, Cleveland, 108 (1952).

2. G. Gottstein and L.S. Shvindlerman, Acta Materialia 50, (2002) 703 (2003).

3. D. Fan, S.P. Chen, L-Q Chen and P.W. Voorhees, Acta Materialia 50, (2002) 1895 (2002).

4. Y. Iijima, N. Tanabe, O. Kohno, and Y. Ikenno, Appl. Phys. Lett. 60, 769 (1992).

5. R. P. Reade, P. Berdahl, S. M. Garrison, and R. E. Russo, Appl. Phys. Lett. 61, 2231 (1992).

6. J. O. Willis, P. N. Arendt, S. R. Foltyn, Q. X. Jia, J. R. Groves, R. F. DePaula, P. C. Dowden, E. J. Peterson, T. G. Holsinger, J. Y. Coulter, M. Ma, M. P. Maley, and D. E. Peterson, Physica C 335, 73 (2000).

7. J. A. Floro, P. G. Kotula, S. C. Seel, and D. J. Srolovitz, Phys. Rev. Lett. 91, 096101-1-4 (2003).

8. R. P. Reade, P. Berdahl, and R. E. Russo, Appl. Phys. Lett. 80, 1352 (2002).

9. P. Berdahl, R. P. Reade, J. Liu, R. E. Russo, L. Fritzemeier, D. Buczek, and U. Schoop, Appl. Phys. Lett. 82, 343 (2003).

10. J. F. Ziegler, SRIM – The Stopping and Range of Ions in Matter, http://www.srim.org/ (2004).

11. K. G. Ressler, N. Sonnenberg, and M. J. Cima, IEEE Trans. on Appl. Superconductivity 7, 1432-1435 (1997).

12. J. Dzick, J. Hoffmann, S. Sievers, L. O. Kautschor, and H. C. Freyhardt, Physica C 372-376, p. 723-728 (2002).

13. W. W. Mullins, J. Appl. Phys. 28, 333-339 (1957).

14. L. Dong and D. J. Srolovitz, Appl. Phys. Lett. 75, 584 (1999).

15. T. Kato, Y. Iijima, T. Muroga, T. Saitoh, T. Hirayama, I. Hirabayashi, Y. Yamada, T. Izumi, Y. Shiohara, and Y. Ikuhara, Physica C 392−396, 790−795 (2003).

16. Work by the German company THEVA and the Technical University of Munich as reported at http://www.theva.com/l.php?r=He4j9GI309523H2P&fr.

17. B. Ma, R.E. Koritala, B.L. Fisher, K.K. Uprety, R. Baurceanu, S.E. Dorris, D.J. Miller, P. Berghuis, K.E. Gray, and U. Balachandran, Physica C 403, 183-190 (2004).

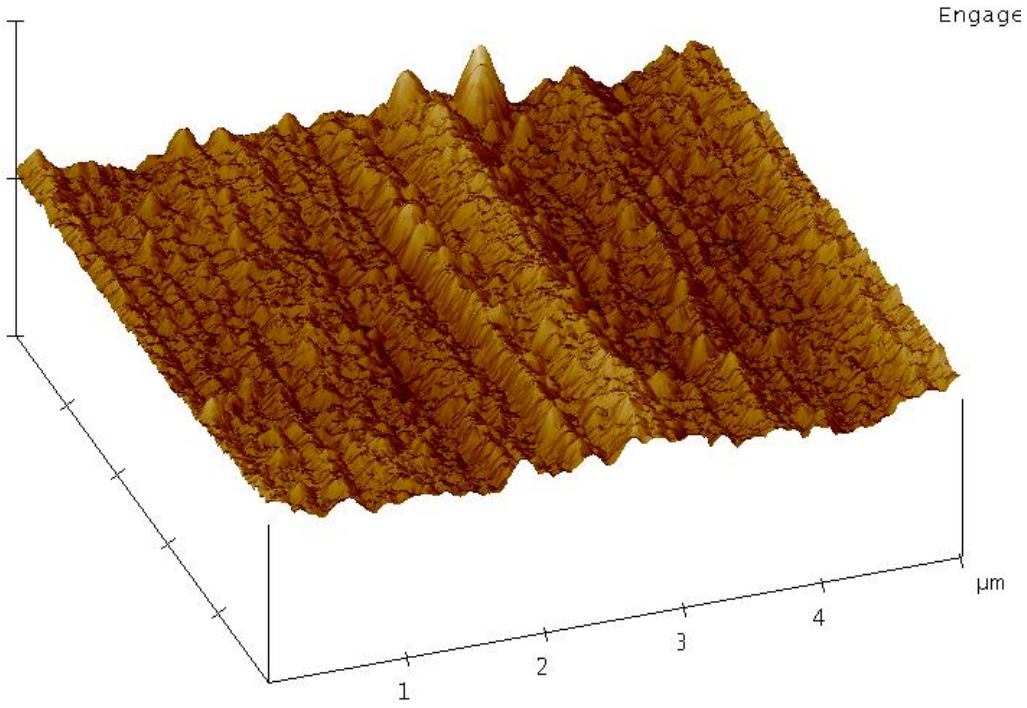

Fig. 1 (a) YSZ film surface after ion bombardment and heating to oxide the film. AFM topograph, 5 µm by 5 µm.; vertical scale 100 nm.

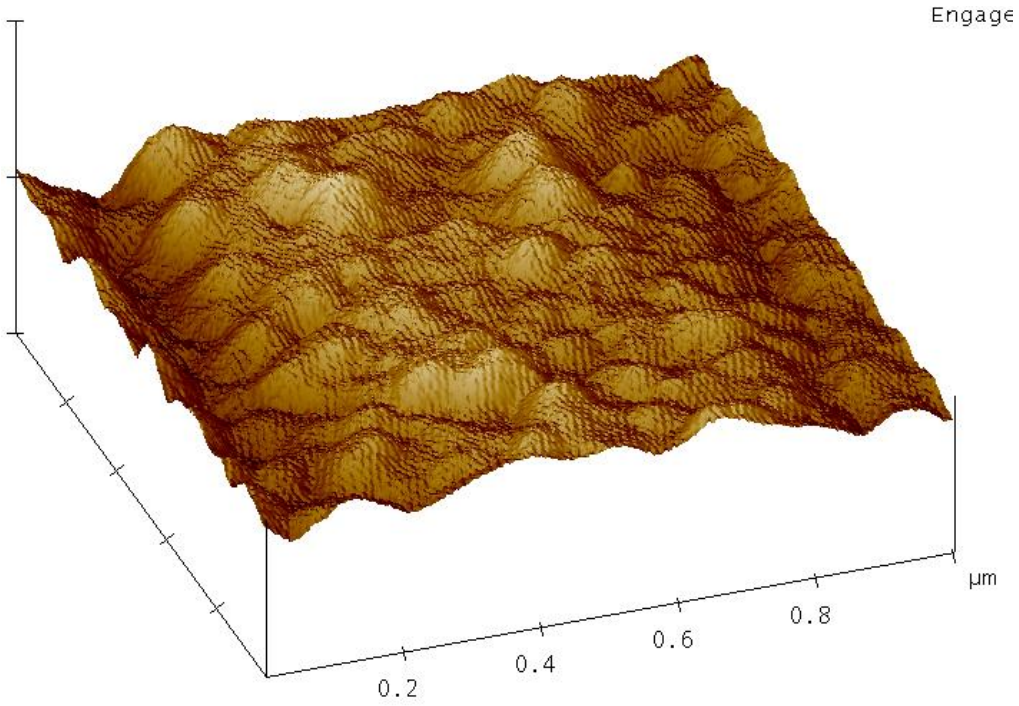

Fig. 1 (b) Closer view of the sample of Fig. 1(a). AFM topograph, 1 µm by 1 µm.; vertical scale 30 nm.

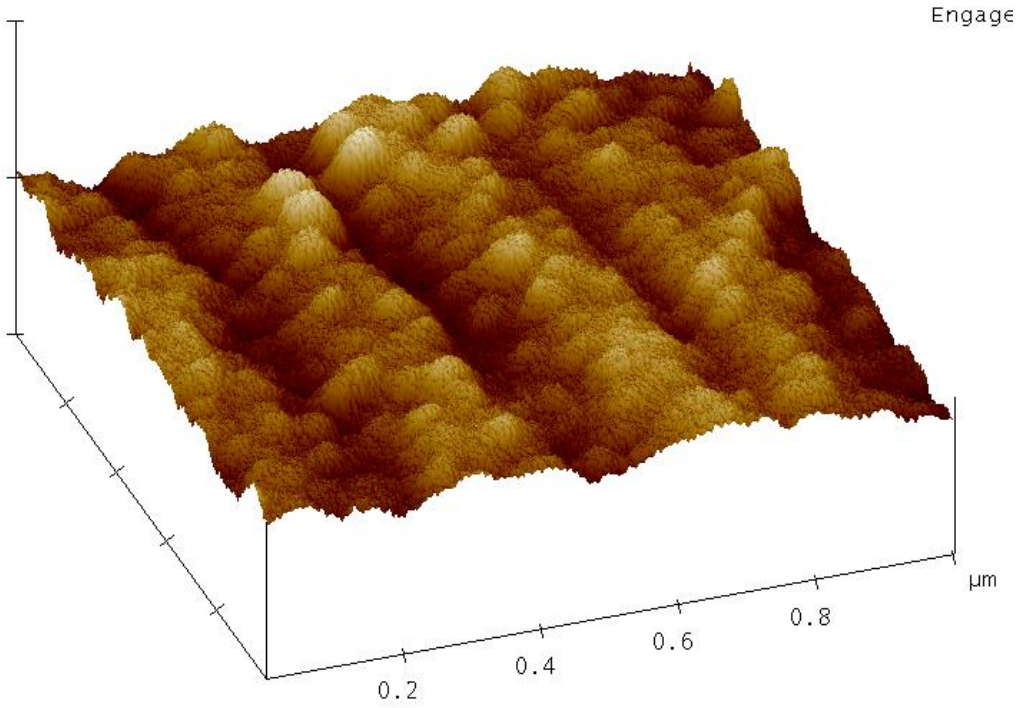

Fig. 2(a) Sample bombarded for 2 min. at room temperature. 1 µm by 1 µm image, vertical scale 30 nm/div.

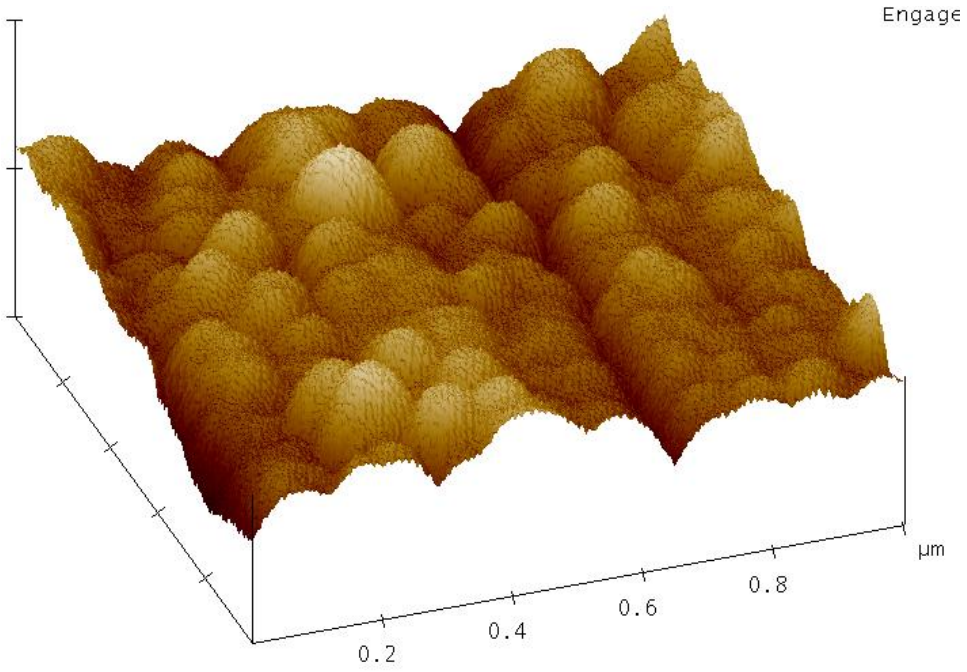

Fig. 2 (b) Sample bombarded for 5 min. at room temperature. 1 µm by 1 µm image, vertical scale 30 nm/div.

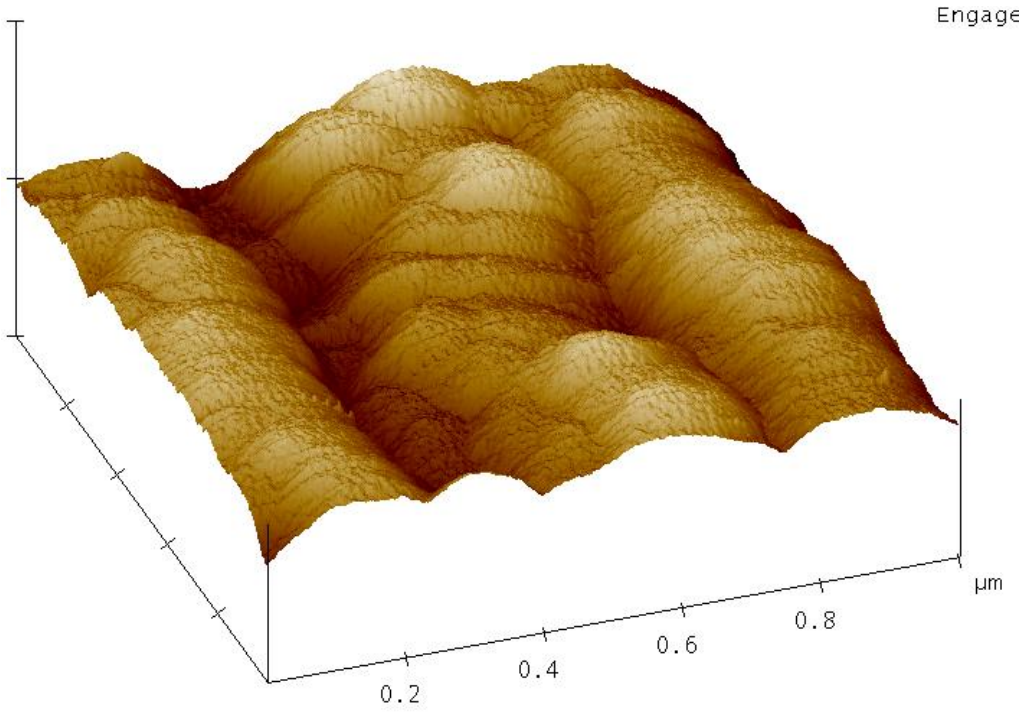

Fig. 2 (c) Sample bombarded for 7.5 min. at room temperature. 1 µm by 1 µm image, vertical scale 30 nm/div.

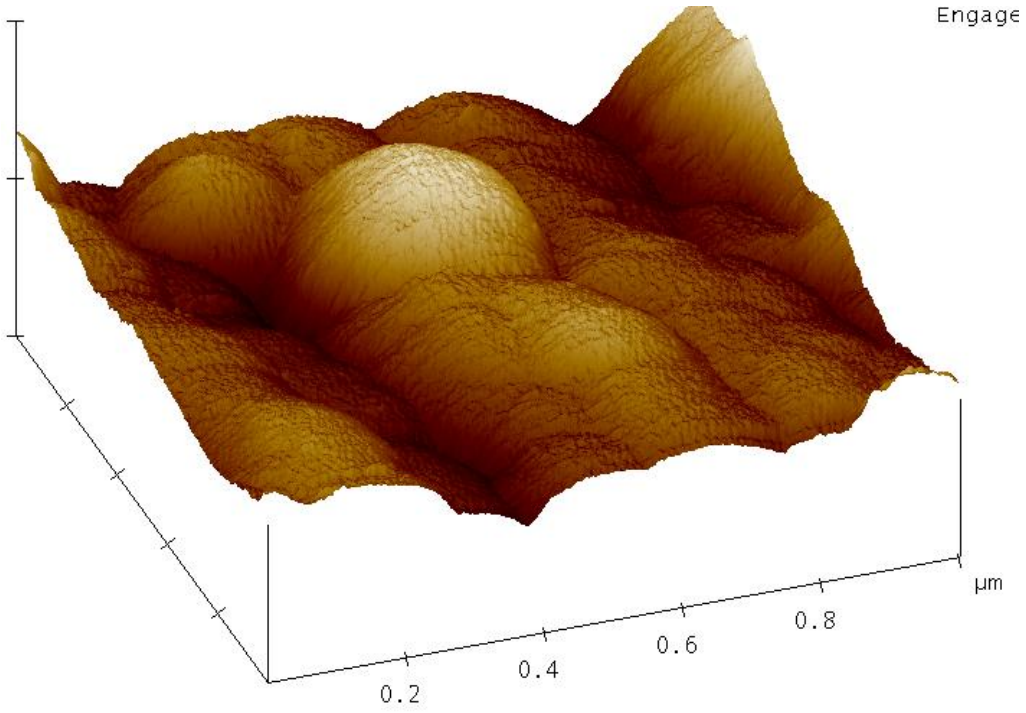

Fig. 2 (d) A second image of the sample bombarded for 7.5 min. at room temperature. 1 µm by 1 µm image, vertical scale 30 nm/div

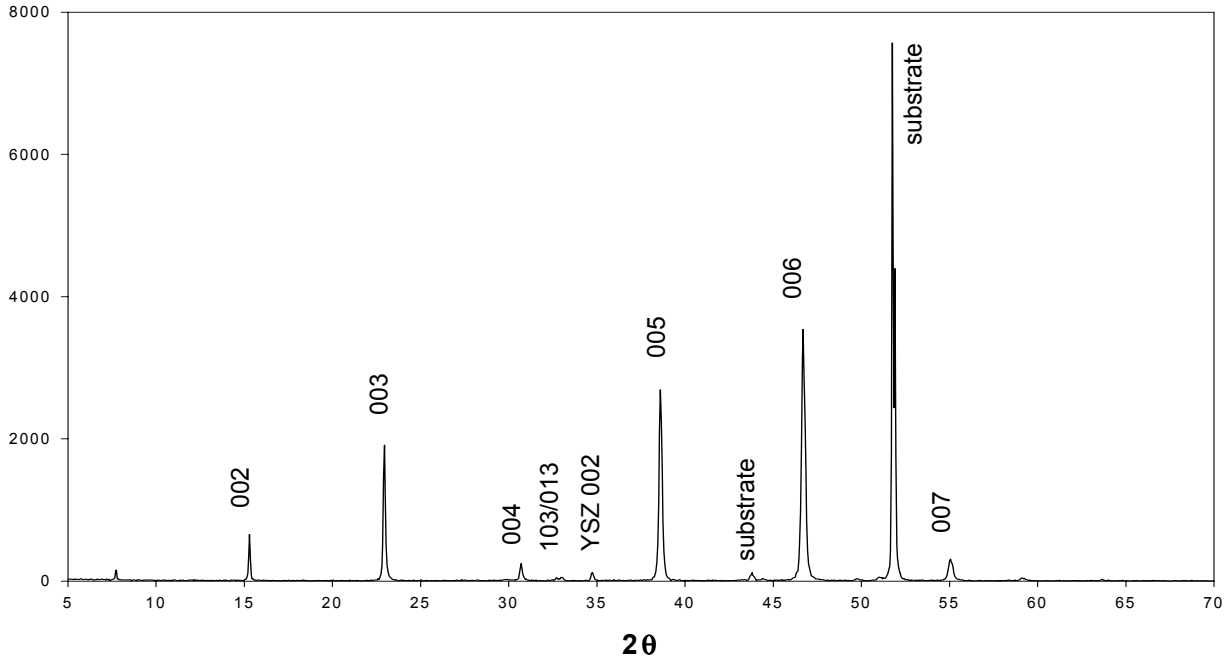

Fig. 3 (a) X-ray diffraction pattern demonstrating that the YBCO c-axis is normal to the film.

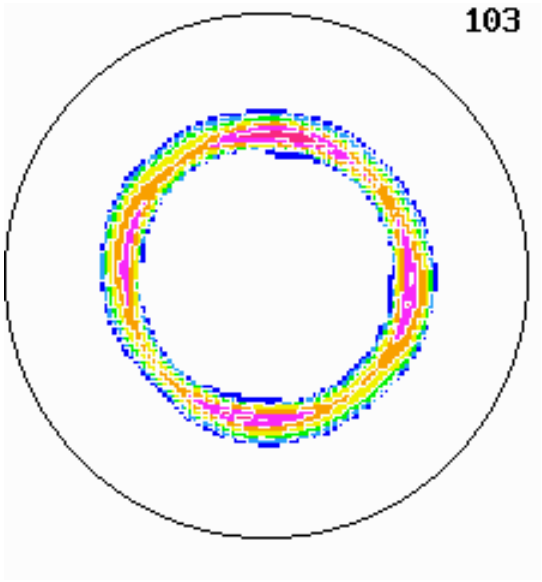

Fig 3 (b) Pole figure for the YBCO (103) pole, confirming that the c-axis is up, and that moderate in-plane texture has been achieved.